Wide-bandgap Zn_2GeO_4 nanowire networks as efficient ultraviolet photodetectors with fast response and recovery time

Chaoyi Yan, Nandan Singh, and Pooi See Lee[a)]
School of Materials Science and Engineering, Nanyang Technological University, 50 Nanyang Avenue, Singapore 639798, Singapore

(Received 13 October 2009; accepted 29 December 2009; published online 2 February 2010)

Ultraviolet (UV) photodetectors based on ternary Zn_2GeO_4 nanowire (NW) networks are demonstrated. The devices show fast response and recovery time, which is attributed to the unique NW-NW junction barrier dominated conductance for network devices. The UV-light induced barrier height modulation is much faster than the oxygen adsorption/desorption processes. The wide-band gap Zn_2GeO_4 NWs also exhibit high wavelength selectivity for deep UV detection. We demonstrate that ternary oxide NW-networks are ideal building blocks for nanoscale photodetectors with superior performance and facile fabrication processes. © *2010 American Institute of Physics*. [doi:10.1063/1.3297905]

Wide-bandgap semiconductor NWs have been widely used as building blocks for nanoscale UV photodetectors.[1–3] Compared with their bulk or thin film counterparts, the nanostructures are expected to exhibit high photosensitivity due to their high surface-to-volume ratios. To date, extensive research has been carried out into binary wide-bandgap materials for UV detection, such as ZnO,[3] SnO_2,[2] ZnS,[4] and GaN.[5] However, much less attention has been paid to more complex materials (such as ternary oxides), probably due to the difficulty in obtaining high quality ternary NWs.[6,7] Especially, no optoelectronic property study of Zn_2GeO_4 NWs has been reported. Ternary oxide NWs are chemically and thermally stable, and are superior for deep UV detection due to their larger bandgap and hence higher wavelength selectivity. For example, ZnO (E_g=3.4 eV) responses to the whole UV band (~200–400 nm), but Zn_2GeO_4 (E_g=4.68 eV) is expected to be UV-A/B (~290–400 nm) blind and only responsive to UV-C band (~200–290 nm).[4] For their potential applications, fast response and recovery time is of great importance but very limited studies have been devoted on the improvement of response and recovery time.[8]

In this letter, we demonstrate the optoelectronic property studies of Zn_2GeO_4 NW network UV photodetectors. Instead of individual NW, the networks are of interest for photodetector fabrication since they yield sufficiently good or even better device performances but only require facile and low-cost lithography techniques.[9,10] Fast response and recovery time within 1 s was observed for all the devices, and this is attributed to the unique NW-NW junction barrier dominated resistance for network devices, which is not available for single-NW devices. Wavelength selectivity was also demonstrated using 254 and 365 nm UV light.

The Zn_2GeO_4 NWs were synthesized via Au-catalyzed vapor-liquid-solid (VLS) mechanism as reported earlier.[11] Mixed ZnO, GeO_2 and carbon powder (molar ratio 2:1:3) was used as source materials and evaporated at 1000 °C for 60 min. The pressure of Ar gas was kept ~2 mbar during heating. Si (100) substrates coated with Au thin film (9 nm) were located at 500–400 °C to collect the NWs. For device fabrication, standard optical-lithography followed by Cr/Au (10/50 nm) deposition and liftoff was used to define the contact electrodes. The Zn_2GeO_4 NWs were suspended in ethanol by sonication (~10 s) and then dispersed on top of the electrodes. UV photoresponse of the devices was characterized by Keithley semiconductor parameter analyzer using a portable UV lamp (254 and 365 nm). All the measurements were performed at room temperature in ambient conditions.

Morphology and crystal structure of the as-grown Zn_2GeO_4 NWs are shown in Fig. 1. A typical top-view scanning electron microscopy (SEM) image of the NWs is shown in Fig. 1(a). The diameters of the NWs are in the range of 10–80 nm, with lengths up to tens of micrometers. All the NWs are single-crystalline, as confirmed by the high-resolution transmission electron microscopy (HRTEM) result shown in Fig. 1(a) inset. X-ray diffraction (XRD) pattern of

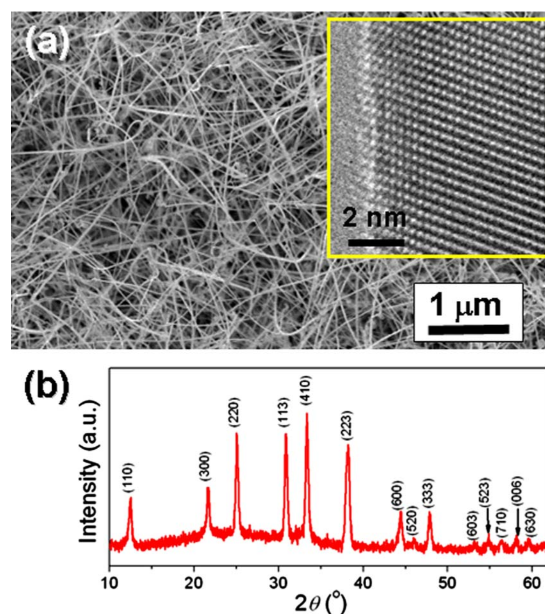

FIG. 1. (Color online) (a) SEM and (b) XRD pattern of the Zn_2GeO_4 NWs grown via Au-catalyzed VLS method. Inset in (a) is HRTEM image of the NW showing the single-crystalline structure. XRD results showed a pure phase of Zn_2GeO_4.

[a)]Author to whom correspondence should be addressed. Electronic mail: pslee@ntu.edu.sg.

 © 2010 American Institute of Physics

Downloaded 21 Apr 2011 to 155.69.4.4. Redistribution subject to AIP license or copyright; see http://apl.aip.org/about/rights_and_permissions

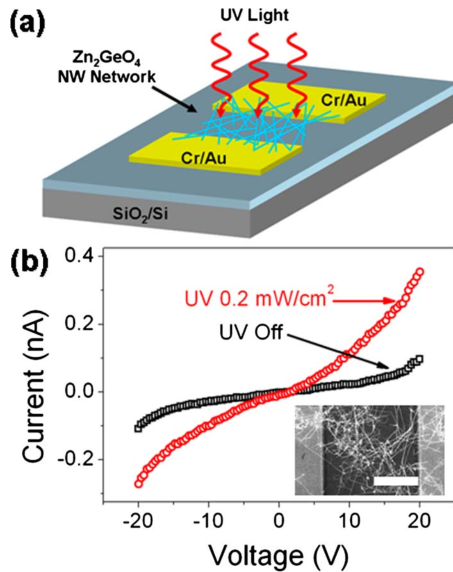

FIG. 2. (Color online) (a) Schematic diagram of the UV photodetector using Zn_2GeO_4 NW networks. (b) *I-V* characteristics of the device in dark (black square) and upon 0.2 mW/cm^2 (red circle) 254 nm UV illumination. Inset is a typical SEM image of the NW network between electrodes. Scale bar is 5 μm.

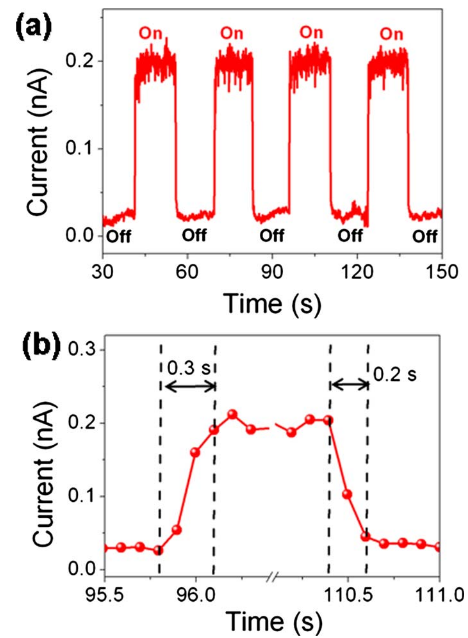

FIG. 3. (Color online) (a) Photoresponse characteristics showing the reversible switching behavior when the 0.2 mW/cm^2 254 nm UV light is turned on and off repeatedly. (b) Enlarged view of a single on/off cycle showing the fast response and reset time within 1 s.

the NWs is shown in Fig. 1(b). All the peaks can be readily indexed to the rhombohedral Zn_2GeO_4 crystal phase. Although impurity phases were usually detected in the vapor phase deposition of ternary oxide NWs,[7,12] no impurity phases such as Ge, ZnO, or GeO_2 were detected in our samples (via a controlled ZnO/GeO_2 molar ratio in the source materials).[11] The high purity Zn_2GeO_4 NWs eliminate the concern that the UV photoresponse may originate from the impurities, such as Ge or ZnO NWs. In contrast to the previously reported short and agglomerated Zn_2GeO_4 nanorods obtained by hydrothermal method,[13] much longer Zn_2GeO_4 NWs can be readily obtained by VLS growth method. The lengths are time-dependent and typically exceed 10 μm for a growth period of 60 min. The high aspect ratio facilitates the photodetector fabrication by connecting the electrodes or forming interconnected NW networks.

The metal-semiconductor-metal photodetector structure is depicted in Fig. 2(a). The Zn_2GeO_4 NW networks are dispersed between the prepatterned Cr/Au electrodes. *I-V* characteristics of the photodetectors measured in dark and under 0.2 mW/cm^2, 254 nm UV illumination are depicted in Fig. 2(b). The *I-V* curves were measured with bias from -20 to 20 V at room temperature in ambient condition. For a fixed bias of 20 V, the current of the NW network increases from 0.09 nA (black square) to 0.35 nA (red circle) when the UV light is turned on. The quasilinear curves indicate that the contact resistance does not contribute significantly when compared with the resistance of the NW network, which is expected to be highly resistant due to the large bandgap (thus extremely low carrier density) and NW-NW junction barriers (details will be discussed below).[7,14]

The photoresponse behavior of the device was characterized by measuring the current as a function of time when the 254 nm UV light was periodically turned on and off, as shown in Fig. 3(a). The measurement bias was fixed at 20 V with UV light intensity at $\sim$0.2 mW/cm^2. A fully reversible switching behavior was observed. The current increased from $\sim$0.02 to 0.2 nA upon UV illumination, which is an enhancement of about tenfold. It is worth noting that the Zn_2GeO_4 NW photodetector exhibited fast response and recovery times within 1 s. An enlarged view of a typical on/off cycle is shown in Fig. 3(b). The measured response and recovery time are 0.3 and 0.2 s, respectively. Similar fast response and reset times ($<$1 s) were observed for all the devices (15 devices measured).

The wavelength selectivity of the Zn_2GeO_4 network devices in UV spectrum was demonstrated using the available 254 and 365 nm UV light. The photoresponse characteristics are shown in Fig. 4(a). The current shows no observable change upon 365 nm UV illumination (black curve), in contrast to the abrupt increase when exposed to 254 nm UV light

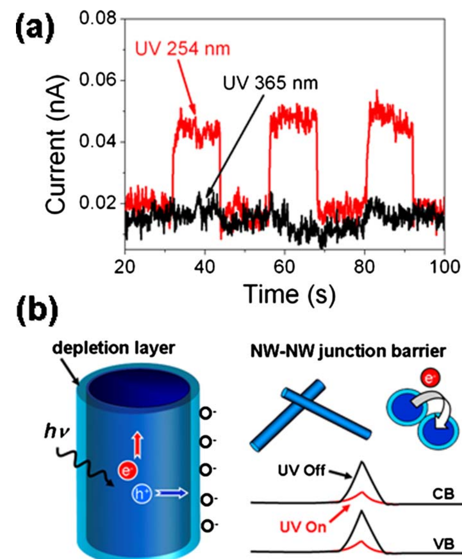

FIG. 4. (Color online) (a) Photoresponse behavior of the device under UV illumination of 254 nm (red line) and 365 nm (black line). (b) Schematic of the carrier generation and NW-NW junction barrier for electron transfer in the network device.

Downloaded 21 Apr 2011 to 155.69.4.4. Redistribution subject to AIP license or copyright; see http://apl.aip.org/about/rights_and_permissions

(red curve). The photon energies of 254 nm UV light (4.88 eV) are high enough to generate electron-hole pairs [$h\nu \rightarrow e^- + h^+$] in the Zn_2GeO_4 NWs (E_g=4.68 eV). However, the increase in carrier density is negligible when exposed to 365 nm UV light with subbandgap photon energies of 3.4 eV and no current increase can be observed [Fig. 4(a)]. This observation reveals that the Zn_2GeO_4 NWs exhibit high wavelength selectivity in the UV-C region, when compared with those extensively investigated binary oxides, such as ZnO and SnO_2.[2,3]

Schematic diagram depicting the carrier generation and transportation processes in the network devices are shown in Fig. 4(b). The UV response and recovery are known to be associated with the oxygen adsorption and desorption processes.[1–3,8] In ambient conditions, oxygen molecules would adsorb on the NW surface by capturing free electrons through $O_2(g) + e^- \rightarrow O_2^-(ad)$, creating a surface depletion layer with low conductivity [Fig. 4(b)]. Carrier density in the NWs increases significantly when illuminated with above-bandgap UV light, by directly exciting electrons from the valence band to conduction band. Adsorbed oxygen ions would be discharged by the photon-generated holes through $O_2^-(ad) + h^+ \rightarrow O_2(g)$, resulting in a reduction in the depletion barrier thickness. Both the increase in carrier density and oxygen desorption contributes to the conductance increase in the NW networks.

For network devices, there is an additional conducting mechanism that is not available in single NW devices. Previously, it has been shown that the resistance of two crossed NWs was dominated by the NW-NW junction barrier, instead of the resistances of the NW themselves.[14,15] In our Zn_2GeO_4 NW network photodetectors, the electrons have to overcome the NW-NW junction barrier when tunneling from one NW to another [Fig. 4(b)]. The electron-transfer barrier originates from the surface depletion layers. As discussed above, the depletion layer can be narrowed by UV illumination due to the increased carrier density, which is equivalent to a lowering of the effective barrier height. It is thus easier for electrons to go through the networks upon UV illumination and therefore resulting in the increase of current (Fig. 3).

In contrast to the previously reported slow response and recovery time,[3,8,16,17] the fast recovery time (<1 s) for our Zn_2GeO_4 NW photodetectors can be attributed to the NW-NW junction barrier dominated conductance. Typically, the NW conductance is still higher than its initial value within a short period upon turning off the UV light, since the oxygen diffusion and readsorption to deplete the NW channel is a slow process.[8,16,17] If the device resistance is dominated by the NW resistance itself (Ohmic contact), a slow current decay to its initial value would be observed. For the NW network structures, the resistance is dominated by the NW-NW junction barriers. The depletion barrier can be treated as two back-to-back Schottky barriers. When the UV light is turned off, the electron-hole recombination would result in a quick increase in the effective barrier height due to the greatly reduced carrier density. The dominate role of the junction barrier would lead to a current decay almost approaching its initial value within a short period (<1 s for our devices). The light induced barrier height modulation is typically much faster than the oxygen diffusion process (on the order of several minutes or hours). For example, it was shown previously that the photocurrent response time for bulk Au-CdS Schottky barrier was typically below 1 s.[18] Very recently, it was also reported that the recovery time of ZnO NW UV-sensors could be improved by focus-ion-beam deposited contacts with Schottky barrier.[8] In this letter, we suggest that the response and recovery time can be enhanced by using NW networks with NW-NW barrier dominated conductance. No intense and expensive lithography processes are required and the single optical-lithography step also allows potential large-scale device fabrication.

In conclusion, we have shown that wide-bandgap Zn_2GeO_4 NWs can be used as efficient UV photodetectors. The network devices showed fast response and recovery time within 1 s, which can be attributed to the NW-NW junction barrier dominant conductance. The large bandgap (4.68 eV) also makes them potential candidates for UV-C detection with high wavelength selectivity. The network-enabled fast response and recovery time as well as facile fabrication processes can be readily extended to other metal oxide nanomaterials.

The authors gratefully acknowledge X. W. Lu, M. F. Lin, M. Y. Chan, S. C. Lim, and J. Guo for their insightful discussions and technical support. C.Y.Y. and N.S. acknowledge the research scholarship provided by Nanyang Technological University, Singapore.

[1] H. Kind, H. Q. Yan, B. Messer, M. Law, and P. D. Yang, Adv. Mater. **14**, 158 (2002).
[2] Z. Q. Liu, D. H. Zhang, S. Han, C. Li, T. Tang, W. Jin, X. L. Liu, B. Lei, and C. W. Zhou, Adv. Mater. **15**, 1754 (2003).
[3] C. Soci, A. Zhang, B. Xiang, S. A. Dayeh, D. P. R. Aplin, J. Park, X. Y. Bao, Y. H. Lo, and D. Wang, Nano Lett. **7**, 1003 (2007).
[4] X. S. Fang, Y. Bando, M. Y. Liao, U. K. Gautam, C. Y. Zhi, B. Dierre, B. D. Liu, T. Y. Zhai, T. Sekiguchi, Y. Koide, and D. Golberg, Adv. Mater. **21**, 2034 (2009).
[5] S. Han, W. Jin, D. H. Zhang, T. Tang, C. Li, X. L. Liu, Z. Q. Liu, B. Lei, and C. W. Zhou, Chem. Phys. Lett. **389**, 176 (2004).
[6] H. J. Fan, Y. Yang, and M. Zacharias, J. Mater. Chem. **19**, 885 (2009).
[7] P. Feng, J. Y. Zhang, Q. Wan, and T. H. Wang, J. Appl. Phys. **102**, 074309 (2007).
[8] J. Zhou, Y. D. Gu, Y. F. Hu, W. J. Mai, P. H. Yeh, G. Bao, A. K. Sood, D. L. Polla, and Z. L. Wang, Appl. Phys. Lett. **94**, 191103 (2009).
[9] H. E. Unalan, Y. Zhang, P. Hiralal, S. Dalal, D. P. Chu, G. Eda, K. B. K. Teo, M. Chhowalla, W. I. Milne, and G. A. J. Amaratunga, Appl. Phys. Lett. **94**, 163501 (2009).
[10] Q. Cao, H. S. Kim, N. Pimparkar, J. P. Kulkarni, C. J. Wang, M. Shim, K. Roy, M. A. Alam, and J. A. Rogers, Nature (London) **454**, 495 (2008).
[11] C. Y. Yan and P. S. Lee, J. Phys. Chem. C **113**, 14135 (2009).
[12] J. S. Jie, G. Z. Wang, X. H. Han, J. P. Fang, Q. X. Yu, Y. Liao, B. Xu, Q. T. Wang, and J. G. Hou, J. Phys. Chem. B **108**, 8249 (2004).
[13] J. H. Huang, X. C. Wang, Y. D. Hou, X. F. Chen, L. Wu, and X. Z. Fu, Environ. Sci. Technol. **42**, 7387 (2008).
[14] X. F. Duan, Y. Huang, Y. Cui, J. F. Wang, and C. M. Lieber, Nature (London) **409**, 66 (2001).
[15] Y. Cui and C. M. Lieber, Science **291**, 851 (2001).
[16] A. Umar, B. K. Kim, J. J. Kim, and Y. B. Hahn, Nanotechnology **18**, 175606 (2007).
[17] S. W. Lee, M. C. Jeong, J. M. Myoung, G. S. Chae, and I. J. Chung, Appl. Phys. Lett. **90**, 133115 (2007).
[18] G. Lubberts, B. C. Burkey, H. K. Bucher, and E. L. Wolf, J. Appl. Phys. **45**, 2180 (1974).

Downloaded 21 Apr 2011 to 155.69.4.4. Redistribution subject to AIP license or copyright; see http://apl.aip.org/about/rights_and_permissions